AN X-RAY EXPERIMENT ON THE PROGNOZ 9 SATELLITE

M. I. Kudryavtsev and S. I. Svertilov

Vestnik Moskovskogo Universiteta, Fizika,
Vol. 39, No. 5, pp. 81-88, 1984

UDC 523.8.08

The Prognoz 9 satellite was launched on 1 July 1983; this is a high-apogee probe, whose basic orbital parameters at the start were as follows: distance from the Earth at apogee 720 thousand km, at perigee 380 km, orbital period 27 days [1]. The axis of rotation was oriented to the Sun, and the period of rotation was about 2 minutes.

The Prognoz 9 apparatus is designed for various space-physics experiments, including research on cosmic X-rays. A major feature of the Prognoz 9 X-ray experiments is that the X-rays are recorded at the same time as charged particles of various types over wide energy ranges. Therefore, one can examine the rises in X-ray background flux due to rises in the charged-particle fluxes, and if necessary one can exclude the simulation of X-ray events by charged particles.

The satellite contains an RKh-1 scintillation spectrometer, which measures X-ray fluxes in the ranges 10-50, 25-50, 50-100, and 100-200 keV [2].

The time resolution of the RKh-1 is determined mainly by the performance of the data-storage and transmission systems. The telemetry system works in two basic states in this experiment.. The first is the permanently active state, in which the readings are taken every 10 sec. The second state is of one reading a second, and this is switched on at those times when the RKh-1 records strong rises in the X-ray fluxes having reasonably steep fronts (solar flares, cosmic gamma bursts, etc.).

The RKh-1 consists of two identical sensors and an electronic circuit. The field of view of each sensor is restricted by appropriate collimators. The direction pattern of each sensor is independent of the azimuthal angle in its own polar coordinate system. The direction pattern is characterized by practically linear decrease over the zenith angle defining the distance of the source from the sensor axis. The maximum zenith angle accepted by the field of view is 51°.

The sensors are located on the instrument panel in such a way that the angle between their axes is 15°, and the axis of rotation of the satellite is the bisector of this angle. As a result, the solar radiation fluxes are recorded during the period of rotation with identical effective areas, while the radiation fluxes from sources deviating from the axis of rotation are modulated with the rotation frequency. The relative modulation amplitude is determined by the angles between the axes of the sensors and the direction to the source.

Various parts of the celestial sphere along the ecliptic fall in the field of view of the instrument because the satellite moves together with the Earth around the Sun.

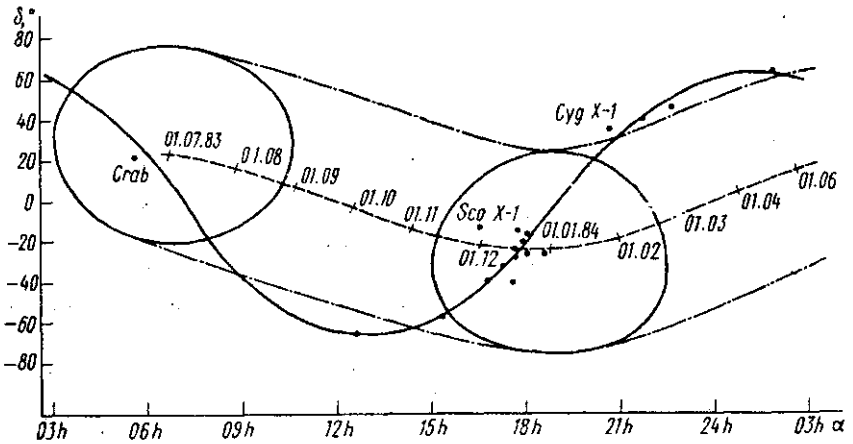

Fig. 1. Path of the field of view of the RKh-1. The dashed line is the path of the center of the field of view. The solid line is the galactic equator. The filled points are the strongest X-ray sources.

Figure 1 shows the path of the field of view in equatorial coordinates for various instants (δ is declination and α is right ascension). The figure also shows the plane of the ecliptic, with the times when the sun is at the corresponding points, and also the plane of the galactic equator.

In the initial flight stage (July-August), the RKh-1 was oriented to the region of the galactic anticenter. The field of view included several X-ray sources, including the strongest one in the hard X-ray range: the source in the Crab nebula. In September-October, the galactic plane did not fall in the field of view. From the start of November, the field of view began to cover the center of the galaxy, where most of the bright X-ray sources are located.

Figure 2 shows major features of the sensor design and the general scheme for the RKh-1. The two sensors are identical in design. The main detecting element in each sensor is a CsI(Tl) scintillator crystal, thickness 2.5 mm, diameter 80 mm.

To reduce the level of the X-ray background and to prevent charged particle being recorded, the sensors in the RKh-1 use a combination of active and passive shielding. The passive shielding includes a lead-tin collimator, as well as lea and barium glass components. The collimator limits the field of view; it consis of a cylinder surrounding the CsI crystal and a grid placed within the cylinder above the crystal. The lead and barium glass components protect the detector from X-rays from the side opposite the collimator. The thicknesses of the glass components and the collimator were chosen such as to provide almost 100% absorption of incident radiation throughout the working energy range: from 10 to 100 keV.

To prevent recording of charged particles and of photons they produce from the passive shielding, the CsI crystal and all the components in the passive shielding, including the collimator, are placed in a container made of plastic scintillator. The thickness of this provides reliable charged-particle recording efficiencies (99%), while the probability of X-ray absorption in the plastic is fairly small in the working energy range. The plastic scintillator and the CsI crystal are viewed by a single photomultiplier from the lead-glass side.

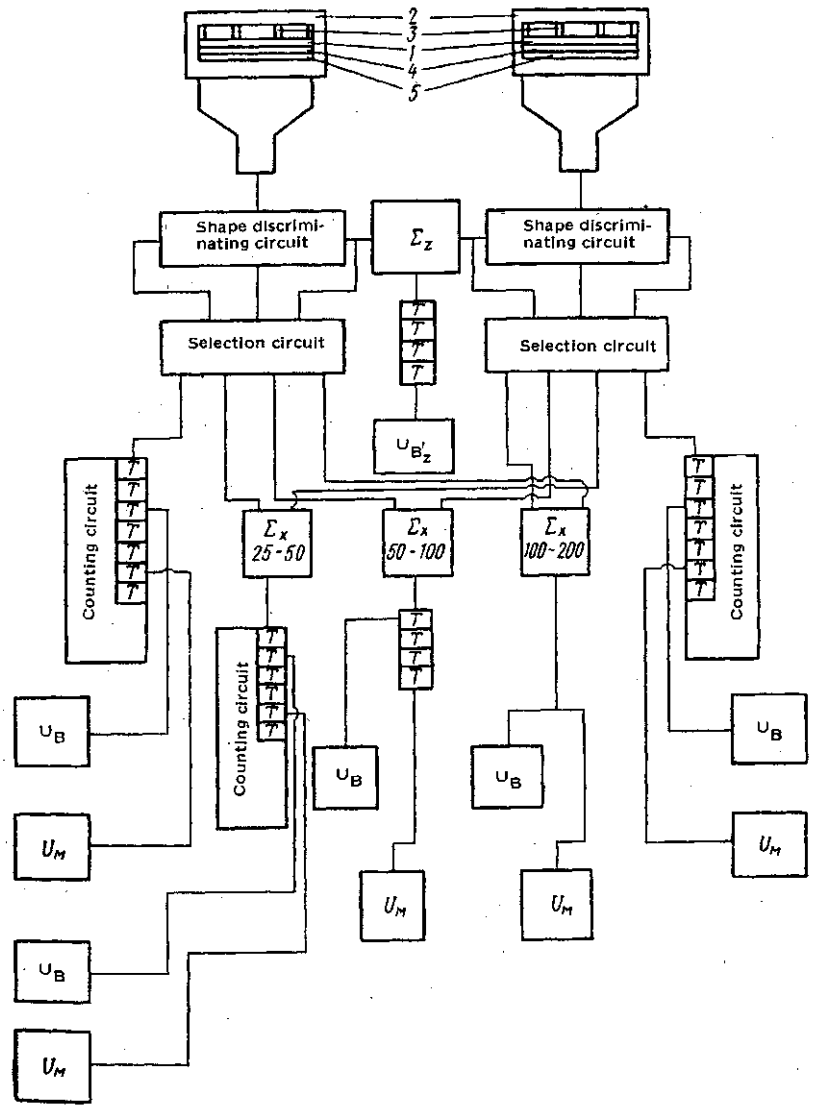

Fig. 2. Functional diagram of the RKh-1: 1) CsI crystal; 2) plastic scintillator; 3) collimator; 4) barium glass; 5) lead glass; T) counting flip-flops.

The pulses from the photomultipliers pass to shape discrimination circuits (Fig. 2), which are used to separate the signals from the plastic scintillator and CsI crystal. The working principle is based on the difference in decay times of the plastic (5 nsec) and the CsI (0.5 μsec). If the pulse reaching the discrimination circuit is short, i.e., is due to an event in the plastic scintillator, the circuit provides logical inhibition. If on the other hand the pulse is longer, the circuit produces an analog signal whose amplitude is proportional to the total charge transported by the current pulse from the photomultiplier.

The signals from the shape discriminators pass to the selection circuits. If the corresponding inputs do not receive the inhibit signal, the selection circuit sorts the pulses by height into one of four channels. The discrimination thresholds are chosen such that these correspond to the following energy

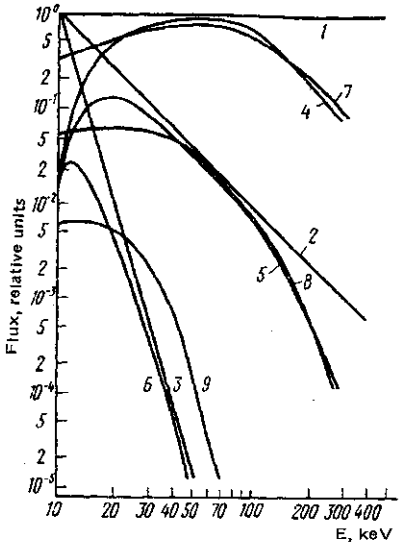

Fig. 3. Curves characterizing the conversion stages in the RKh-1: 1-3) initial spectra (1 E^0, 2 E^{-2}, 3 E^{-7}); 4-6) corresponding secondary-electron spectra; 7-9) pulse-height spectra expressed in energy units.

ranges: 10-50, 25-50, 50-100, and 100-200 keV. The signals from both sensors are summed in the corresponding Σ_x cells for the ranges 25-50, 50-100, and 100-200 keV.

The numbers of counts in unit time are recorded by the logarithmic ratemeters U_B and U_M, which differ in time-constant: τ_{U_B} = 1.5 sec and τ_{U_M} = 10 sec. There are also counting circuits for the pulses in the ranges 10-50 and 25-50 keV. There are two types of logarithmic ratemeters because of the two interrogation rates in the telemetry system.

The inhibit signals from the shape discriminators are summed in the Σ_z cells, and the number in unit time is measured by the logarithmic ratemeter U_{B_z}.

When X-ray quanta enter a detecting element, the photoelectric and Compton interactions result in much of the energy being given to secondary electrons, whose energy is converted to scintillations, which produce current pulses in the photomultiplier.

The first stage in the initial spectrum conversion is governed by the energy dependence of the recording efficiency, i.e., the probability of energy transfer from the X-ray quanta to electrons, while the second stage is governed by the pulse-height distribution from the photomultiplier corresponding to a certain energy deposition in the crystal.

The pulse-height distribution from the photomultiplier in the RKh-1 can be represented by a Gaussian distribution whose variance is dependent on energy. The relative width of this distinction at half height is a measure of the energy resolution. Measurements show that the resolution increases as the energy decreases and becomes more than 100% at 10 keV.

These transformations were calculated for several spectra characterized by

decreasing intensity as the energy increases. Figure 3 shows curves for initial spectra of power-law form: steep (exponent α, for example, of 7, as in curve 3), less steep ($\alpha = 2$, curve 2), and uniform ($\alpha = 0$, curve 1).

Curves 4-6 are the secondary-electron spectra corresponding to the initial X-ray spectra of curves 1-3. Curves 7-9 are the pulse-height spectra at the photomultiplier anode.

Figure 3 shows that the recording efficiency (curve 4) varies most rapidly in the range 10-30 keV, as it increases with energy. This is due to the absorption of the X-rays in the plastic scintillator increasing at low energies because of increase in the interaction cross section. There is little change in efficiency in the range 30-100 keV, but above 100 keV a fall sets in because of the reduction in the interaction cross section in the CsI crystal.

The energy dependence of the efficiency has the largest effect on the steep ($\beta > 5$) spectra, where much of the energy lies in the range below 30 keV (curve 6 in Fig. 3). Less steep spectra ($\beta = 1.5$-5) are less distorted, and their shape is in principle retained in the basic recording range (30-150 keV). Even less steep spectra ($\beta < 1.5$) are substantially distorted in the high-energy range (>150 keV).

The effects of the real energy resolution on the spectrum transformation are illustrated by the differences in the pairs of curves 4-7, 5-8, and 6-9. The steep spectra are the most affected.

The spectral information is represented by integral quantities (count rates) at the circuit output.

Some assumptions must be made about the shapes of the initial spectra to determine the spectral and angular characteristics of the fluxes from the count rates. For example, if the initial spectra are of power-law form or of the form given by an optically thin plasma, one can use the ratios of the over-all count rates in various energy ranges to determine the exponent β (for power-law spectra) or the effective temperature kT (for spectra of optically thin plasma type).

The count rates from the two sensors in the range 10-50 keV enable one to determine the angles between the axes of the detectors and the direction to the source. If we know these angles and the parameters β or kT, the over-all count rates can be used to determine the fluxes in the corresponding energy ranges.

During the first half-year of flight (from 1 July 1983 through 1 January 1984), the RKh-1 recorded several hundred bursts of solar X-rays. Figure 4a shows the time course of the count rates in the various ranges for one of these bursts on 16 October 1983. Figure 4b indicates the spectrum dynamics in this event. The above method was used to determine β in the power-law approximation for various instants for the energy range 25-100 keV.

Promising preliminary results were obtained also on cosmic gamma bursts (not of solar origin) and with X-ray pulsars. The data are at present being processed, but the scope for experiments on these can be evaluated on the basis of the observation time and the background conditions.

We estimate the sensitivity of the RKh-1 in recording X-ray bursts. The background count rates in the most suitable energy ranges 25-50 and 50-100 keV are correspondingly, 22 and 19 count/sec. An increase in count rate is considered as reliably detected if it exceeds the background by more than three times the standard deviation. If one assumes that a typical X-ray burst has the dura-

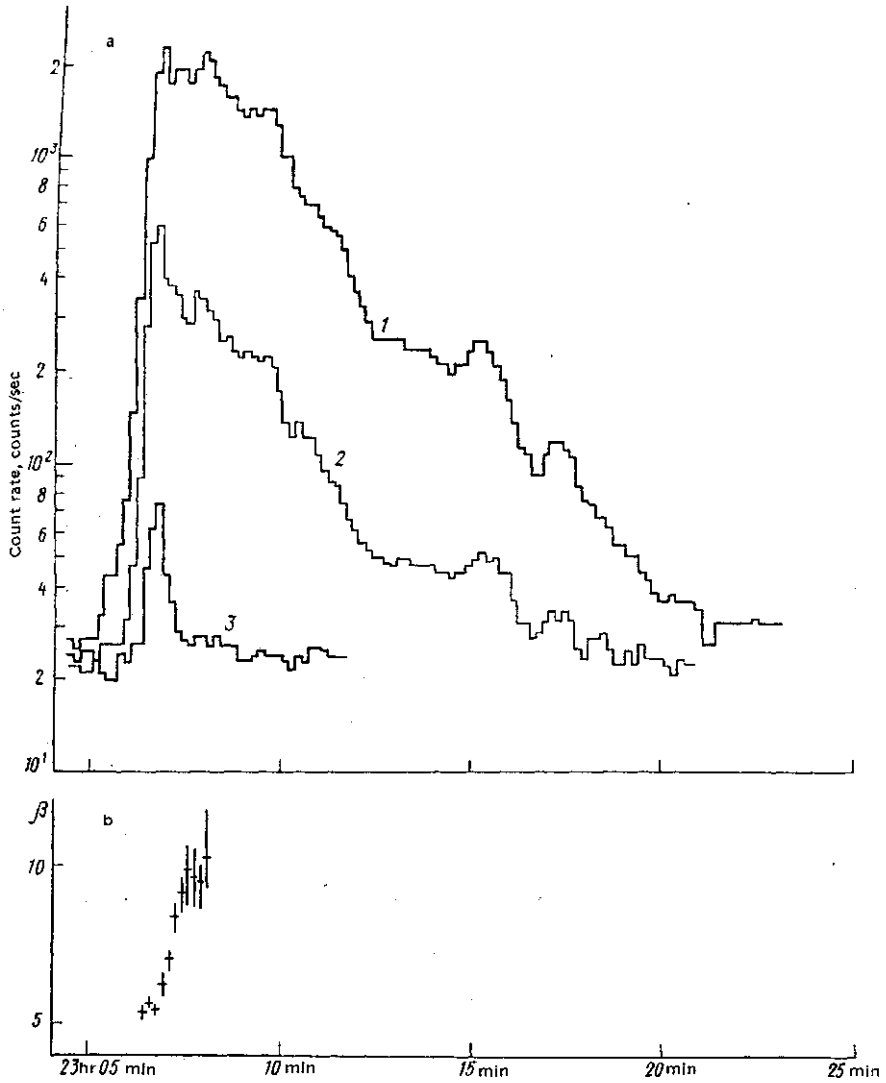

Fig. 4. a) Time dependence of the count rates in the flare of 16 October 1983: 1) range 10-50 keV; 2) 25-50 keV; 3) 50-100 keV (Moscow time); b) time dependence of the spectral index β in the burst of 16 October 1983.

tion of 10 sec and a spectrum of optically thin plasma type having kT = 50 keV, the energy in the weakest burst that can be recorded with the RKh-1 is ~$2.5 \cdot 10^{7}$ erg·cm^{-2}.

In the case of gamma burst recording, the sensitivity characteristic of the RKh-1 is of the same order as that in the Konus apparatus [3] used with the Venus-11, 12, 13, and 14 probes, which gave the best data on the burst statistics. If on the other hand the sensitivity measure is taken as the energy deposition in unit time, the corresponding quantity for the RKh-1 is $2.5 \cdot 10^{-8}$ erg·cm^{-2}·sec^{-1} for typical gamma bursts (with duration 10 sec and kT = 50 keV), which is less by an order of magnitude than the characteristic for the Konus apparatus [4].

When one records radiation from periodic X-ray sources, the exposure time is a major characteristic. The field of view of the RKh-1 is such that the maximum observation time for a given source under favorable conditions is ~100 days. With the above values for the background count rates, the exposure time of 100 days provides a relative error in measuring the count rate of $\sim 10^{-4}$. If one assumes that a typical X-ray source has a power-law spectrum with exponent ~3, the weakest fluxes from such sources that can be recorded with the RKh-1 are as follows: $\sim 3 \cdot 10^{-5}$ quantum$\cdot$cm$^{2}\cdot$sec$^{-1}\cdot$keV^{-1} at 25 keV, and $\sim 3 \cdot 10^{-6}$ quantum$\cdot$cm$^{2}\cdot$sec$^{-1}\cdot$keV^{-1} at 50 keV.

For comparison we note that typical hard X-ray sources recorded at present have fluxes of $\sim 10^{-3}$-10^{-4} quantum$\cdot$cm$^{-2}\cdot$sec$^{-1}\cdot$keV^{-1} at 29-30 keV [5,6].

Therefore, the RKh-1 can provide new data also on periodic X-ray sources.

REFERENCES

1. Pravda, 3 July 1983.
2. Yu. P. Gordeev and M. I. Kudryavtsev, in: New Instruments, Devices, Methods, Materials, and Technological Processes Developed by Moscow University Scientists and Proposed for Introduction into the Economy and Science [in Russian], p. 36, Izd. MGU, Moscow, 1982.
3. E. P. Mazets and S. V. Golenetskii, in: Astrophysics and Space Physics [in Russian], p. 216, Nauka, Moscow, 1982.
4. E. P. Mazets et al., Pis'ma v Astron. Zh., vol. 6, p. 609, 1980.
5. J. F. Dolan et al., Astrophys. J., vol. 250, p. 355, 1981.
6. W. Pietsch et al., Astrophys. J., vol. 237, p. 964, 1980.

27 December 1983

Nuclear Physics Research Institute